

AD-AOPF 538

RIA-80-U770

TECHNICAL LIBRARY

AD

A088538

TECHNICAL REPORT ARLCB-TR-80025

A PHOTOELASTOPLASTIC STUDY OF STRESS CONCENTRATION FACTORS AND RESIDUAL STRESSES IN TWO NOTCHED SPECIMENS OF POLYCARBONATE MATERIAL

Y. F. Cheng

July 1980



US ARMY ARMAMENT RESEARCH AND DEVELOPMENT COMMAND
LARGE CALIBER WEAPON SYSTEMS LABORATORY
BENÉ WEAPONS LABORATORY
WATERVLIET, N. Y. 12189

AMCMS No. 36KA7000204

DA Project No. 156401813GRN

PRON No. 1A0215641A1A

APPROVED FOR PUBLIC RELEASE; DISTRIBUTION UNLIMITED

DISCLAIMER

The findings in this report are not to be construed as an official Department of the Army position unless so designated by other authorized documents.

The use of trade name(s) and/or manufacturer(s) does not constitute an official indorsement or approval.

DISPOSITION

Destroy this report when it is no longer needed. Do not return it to the originator.

(BLOCK 20 CONTINUED)

state, stress concentration factors are readily applicable to specimens of any material with similar geometry and loading. In the elastoplastic state, it requires the similarity of stress-strain relation between model and prototype materials.

TABLE OF CONTENTS

	<u>Page</u>
ACKNOWLEDGEMENT	iii
INTRODUCTION	1
EXPERIMENTAL METHOD	1
NOMINAL STRESS	4
EXPERIMENTS AND RESULTS	6
Apparatus	6
Material and Calibration	6
Model and Loading	9
Maximum Shear Stress Distribution Across Section AB	9
Elastic Plastic Boundary	12
Boundary Stresses and Stress Concentration Factors	12
DISCUSSIONS	16
Calculated Residual Stress and Percentage of Overloading	16
Stress at Point B in C-Shaped Specimens	18
Transition to Prototype	18
CONCLUSIONS	19
REFERENCES	20

TABLES

I. SIZE OF PLASTIC REGION	13
II. STRESS CONCENTRATION FACTOR, PERCENTAGE OF OVERLOADING, AND RESIDUAL STRESS IN C-SHAPED SPECIMEN	14
III. STRESS CONCENTRATION FACTOR, PERCENTAGE OF OVERLOADING, AND RESIDUAL STRESS IN THE COMPACT TENSILE SPECIMEN	15

ILLUSTRATIONS

	<u>Page</u>
1. Sketch of C-shaped specimen.	2
2. Sketch of compact tensile specimen.	3
3. Sketch for deriving nominal stresses.	5
4. Stress-fringe curve for polycarbonate.	7
5. Stress-strain curve for polycarbonate.	8
6. Maximum shear stress distribution across section AB in C-shaped specimen.	10
7. Maximum shear stress distribution across part of section AB in compact tensile specimen.	11
8. Curves of stress concentration factor, K , and maximum boundary stress, σ_{\max} , versus nominal stress, σ_{nom} .	17

ACKNOWLEDGEMENT

Charles Cobb's participation in the experimental phase of this investigation is hereby acknowledged.

INTRODUCTION

Results obtained by another section of this laboratory in testing a notched C-shaped specimen, Figure 1, and a notched compact tensile specimen, Figure 2, showed that an increase of initial tensile overload is accompanied by an increase of fatigue life of the specimen. This can be explained by the well-known fact that a tensile overload produces a compressive residual stress upon unloading. Thus, an increase of overload increases the residual stress which reduces the nominal stress in a fatigue test and improves the fatigue life.

This report describes a photoelastoplastic study on stress concentrations, in elastic as well as in elastoplastic states, and residual stresses after unloading in both specimens. The principles of experimental method are outlined, equations for nominal stresses are given, and stress concentration factors are found. In the elastic state, these values are readily applicable for specimens made of any material with similar geometry and loading. In the elastoplastic state, transition of data requires the similarity of stress-strain relation between model and prototype materials.

EXPERIMENTAL METHOD

The photoelastic stress analysis is based on the linear stress-optic law.¹ The discovery of the non-linear stress-optic law extends the photo-

¹Frocht, M. M., Photoelasticity, Vol. I and II, John Wiley and Sons, 1948.

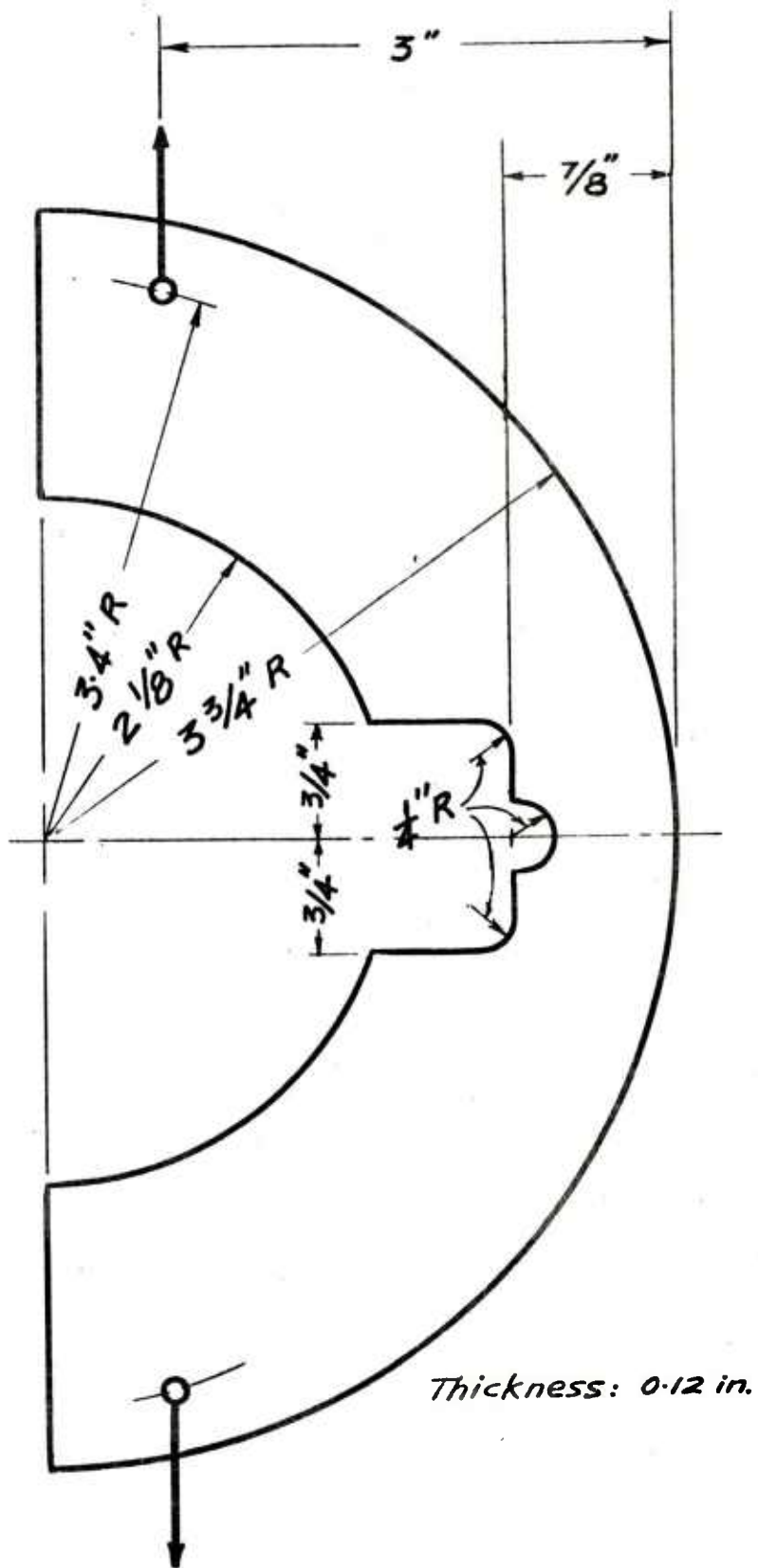
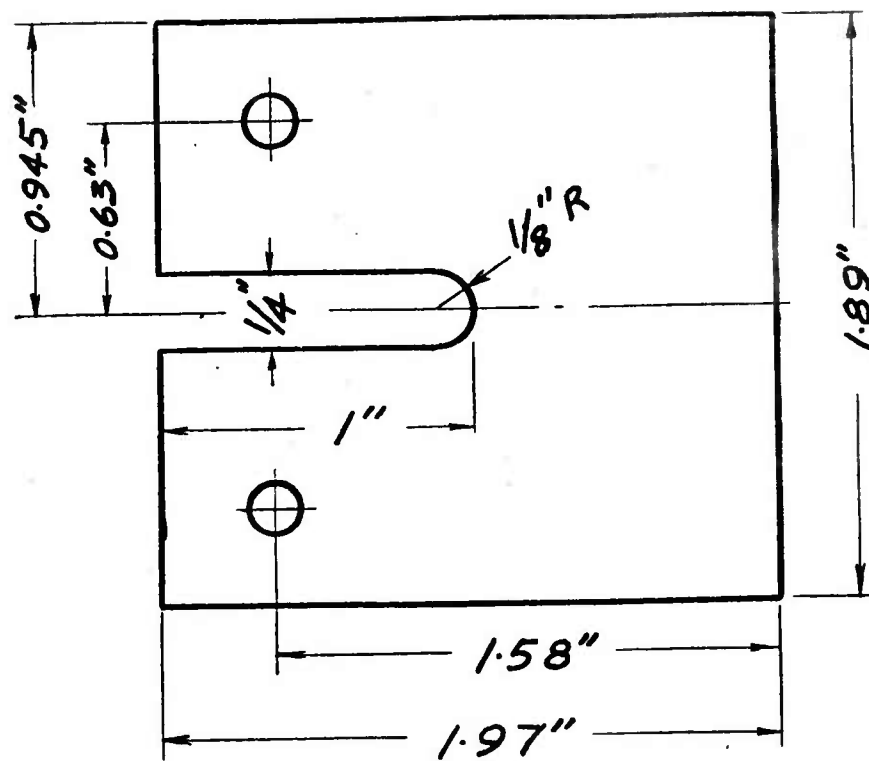


Figure 1, Sketch of C-Shaped Specimen,



Thickness: 0.12 in.

Figure 2. Sketch of Compact Tensile Specimen.

elastic method to the plastic range.² Specifically, at any point in a model, whether elastic or plastic, the fringe order N is related to the principal stress difference $(\sigma_p - \sigma_q)$ by a calibration curve, and the isoclinic parameter gives directly the directions of the principal stresses σ_p and σ_q .

In this investigation, we are interested only in the boundary stress and maximum shear stress. No attempts were made to determine the individual stress distribution, although techniques are readily available.

On the free boundary one of the principal stresses is identically zero, and the remaining principal stress tangent to the boundary is given by the fringe order N .

It can be shown from Mohr's circle that the maximum shear stress, τ_{\max} , equals one-half of the principal stress difference; i.e., $\tau_{\max} = (\sigma_p - \sigma_q)/2$.

For a material obeying the yield condition of maximum shear stress, the position of elastic-plastic boundary is given by the particular fringe order having a maximum shear of $\sigma_y/2$, where σ_y is the tensile yielding stress.

NOMINAL STRESS

Superposing the given load P with an identical pair of load acting at the centroid of the cross section AB and parallel with the given direction as shown in Figure 3, an equivalent loading system is obtained. It consists of a moment PR and a tensile load P where R denotes the distance between two

²Frocht, M. M. and Cheng, Y. F., "An Experimental Study of the Laws of Double Refraction in the Plastic State in Cellulose Nitrate - Foundations for Three Dimensional Photoplasticity," Proceedings International Symposium on Photoelasticity, pp. 195-216, 1961.

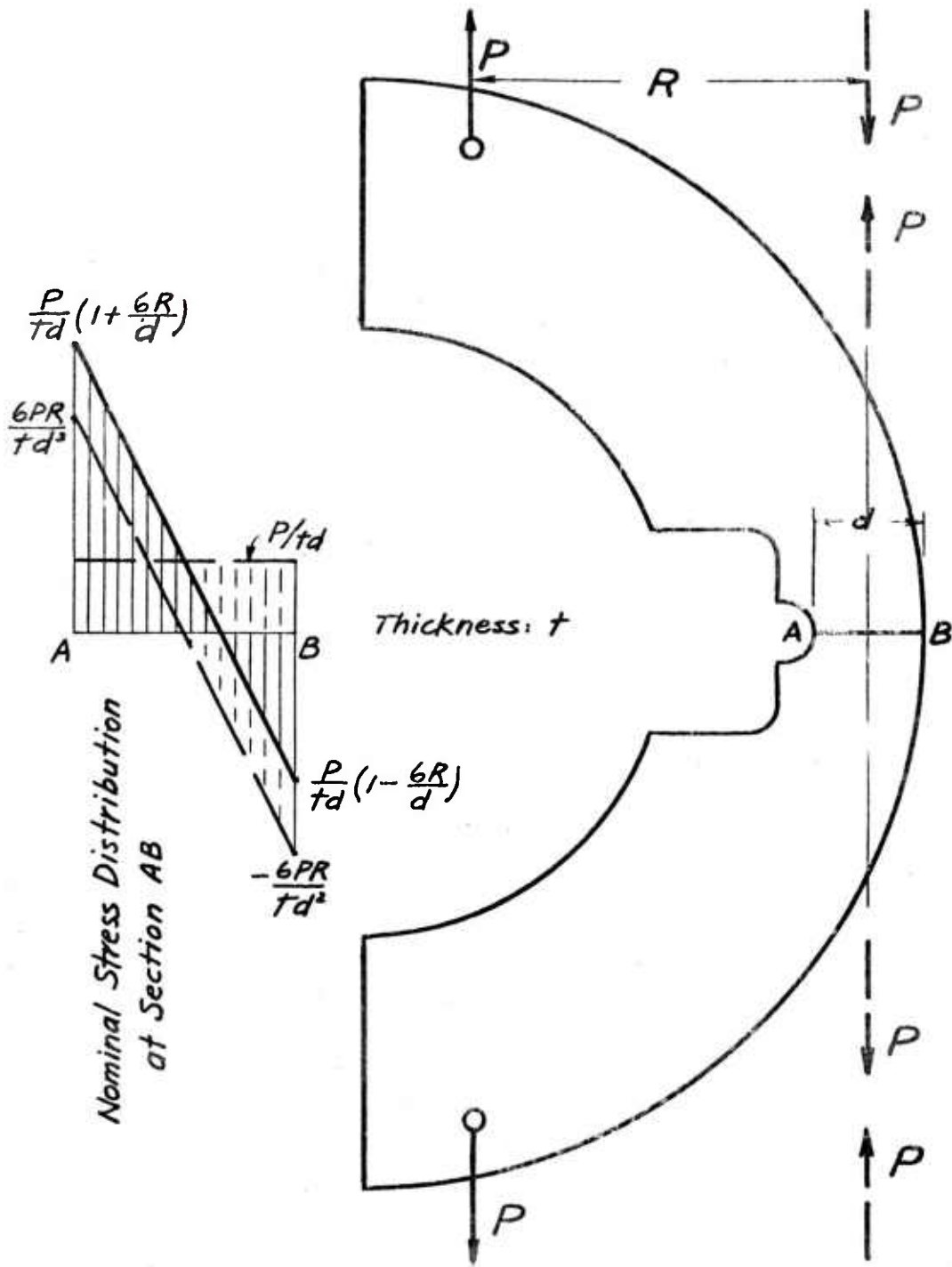


Figure 3. Sketch for Deriving Nominal Stresses.

load lines i.e., the original and the superposed loads. The nominal stress due to bending is $6PR/td^2$ and that due to tension is P/td , where t denotes the thickness and d the width of section AB. The nominal stress at A and B, σ_{An} and σ_{Bn} , is equal to the sum and difference of the stress due to bending and tension, respectively. Thus

$$\begin{aligned}\sigma_{An} &= \frac{P}{td} \left(1 + \frac{6R}{d}\right) \\ \sigma_{Bn} &= \frac{P}{td} \left(1 - \frac{6R}{d}\right)\end{aligned}\tag{1}$$

It can be seen that the above expressions hold also for compact tensile specimen.

EXPERIMENTS AND RESULTS

Apparatus

A lens type transmission polariscope with collimated monochromatic light of 5461 \AA was used, and photoelastic patterns at normal incidence were observed through a telemicroscope of 7.2X. Static loads were applied through a dead weight loading frame having a lever ratio of 4.

Material and Calibration

A sheet of LEXAN, a polycarbonate resin manufactured by the General Electric Company, of 0.12 inch thickness was used as model material. Figures 4 and 5 show the stress-fringe and stress-strain curves obtained from calibration at a temperature of $73^\circ \pm 3^\circ\text{F}$ and a relative humidity of $10\% \pm 5\%$. It has an elastic fringe value of 36 psi per inch, Young's modulus E of 3.25×10^5 psi, proportional limit of approximately 6.2×10^3 psi, and secant yield strength, σ_1 , defined by the point of intersection of secant

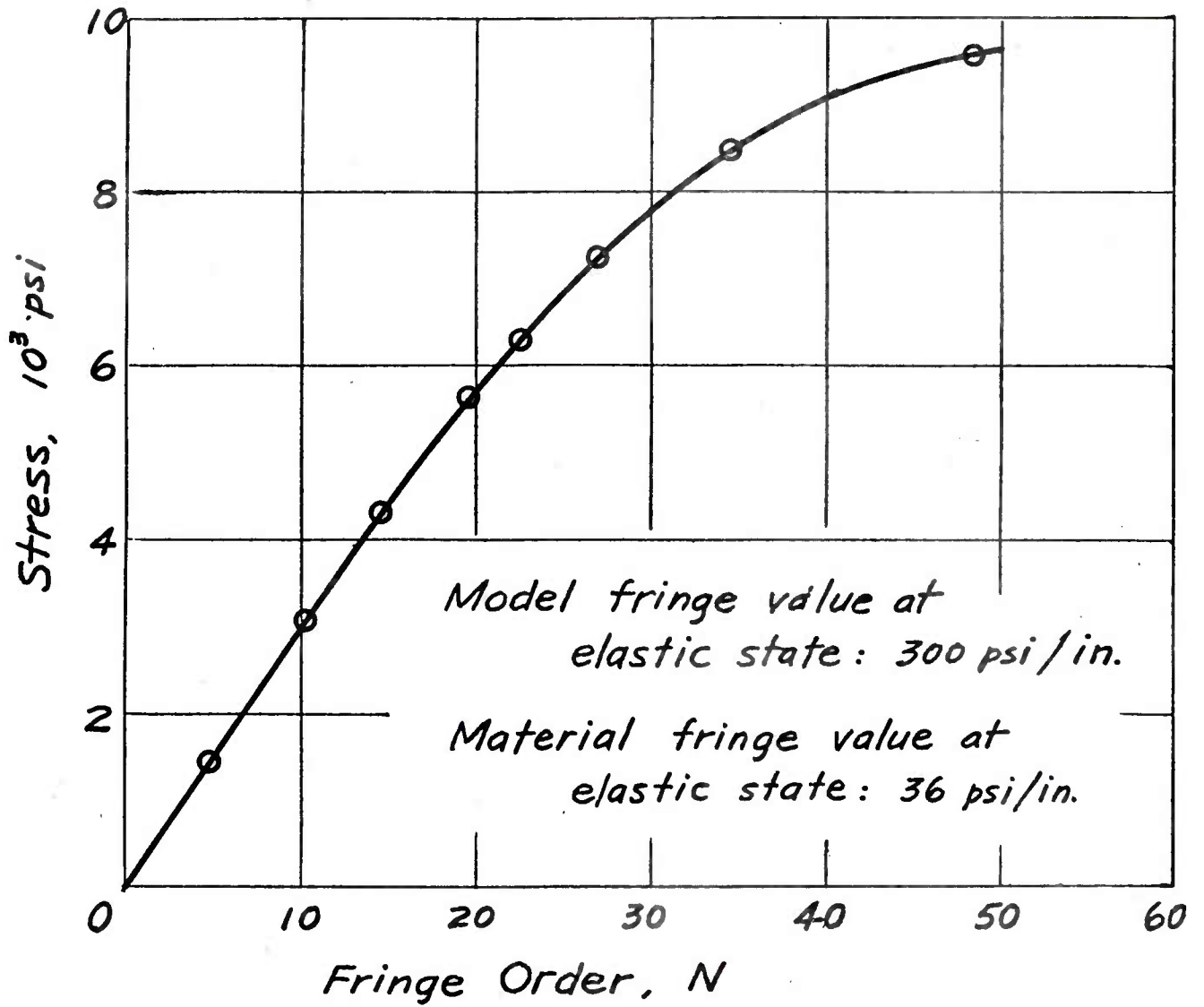


Figure 4. Stress-Fringe Curve for Polycarbonate.

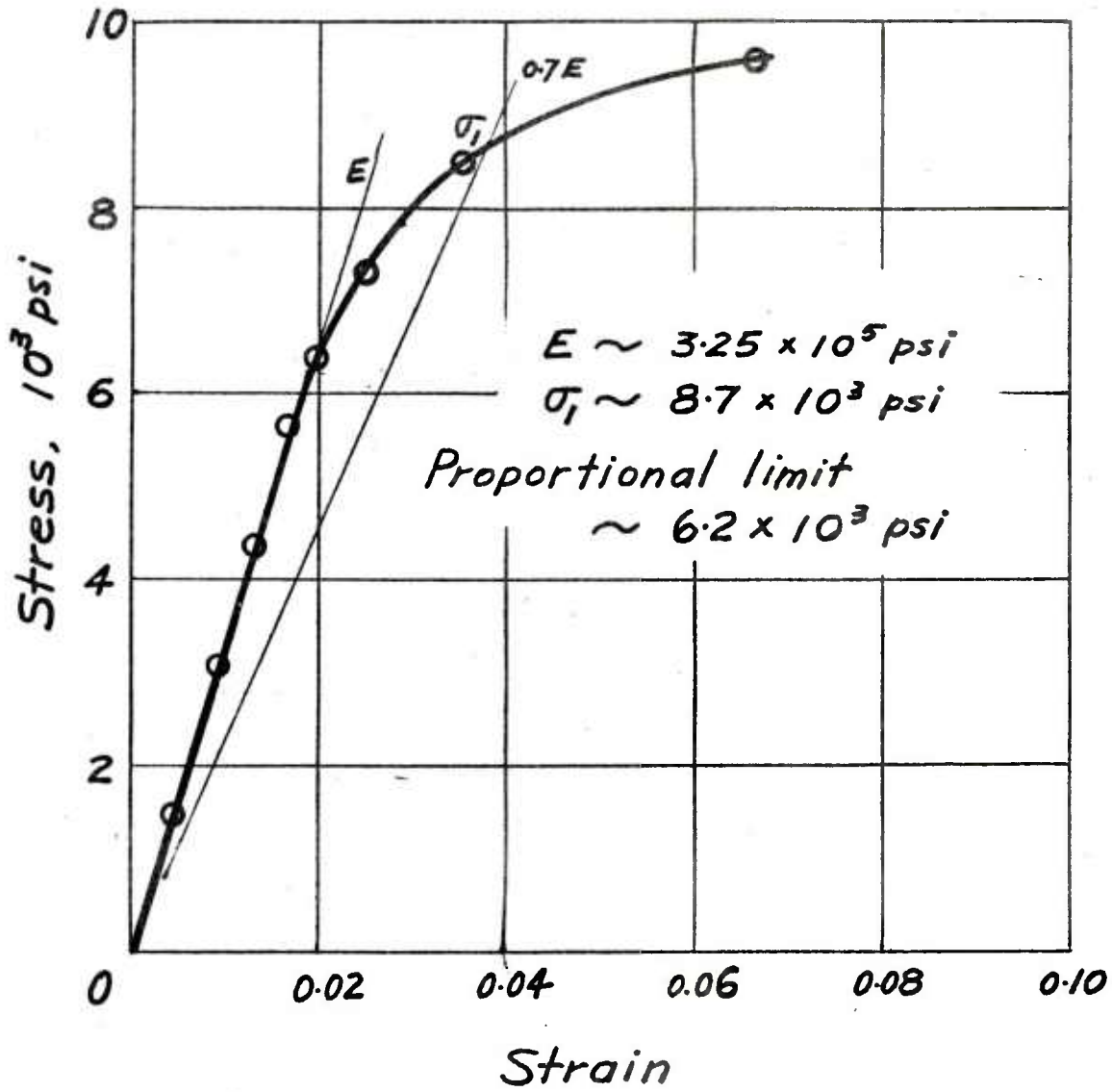


Figure 5. Stress-Strain Curve for Polycarbonate.

modulus ($E_{\text{sec}} = 0.7E$) and the stress-strain curve, of approximately 8.7×10^3 psi. Luder's lines have been observed during calibration indicating that this material follows maximum shear stress yield criterion.

The Ramberg-Osgood equation³ for this material has the following form

$$\frac{E\varepsilon}{\sigma_1} = \frac{\sigma}{\sigma_1} + \frac{3}{7} \left(\frac{\sigma}{\sigma_1}\right)^{11.5}$$

where ε denotes strain, σ stress, and σ_1 secant yield strength.

For details of calibration procedure, see Reference 4.

Model and Loading

Three full scale models each of the C-shaped and compact tensile specimen, Figures 1 and 2, were made of 0.12 inch thick LEXAN plate. In order to minimize any effect of material homogeneity, they were cut closely to the calibrations specimens with their lines of loading parallel to each other. One model was tested in the elastic state. The other two models were tested in the elastoplastic state. Each elastoplastic test requires a fresh model. The load was applied through pins as shown in the sketch.

Maximum Shear Stress Distribution Across Section AB

Photographs of the isochromatic fringe pattern were taken at each load. The fringe distribution across section AB was determined and converted into maximum shear stress according to the stress-fringe relation, Figure 4. The results are shown in Figures 6 and 7.

³Ramberg, W. and Osgood, W. R., "Description of Stress Strain Curves by Three Parameters," NACA TN 902, 1943.

⁴Cheng, Y. F., "A Photoplastic Study of Residual Stress in an Overloaded Breech Ring," Technical Report ARLCB-TR-78018, Benet Weapons Laboratory, LCWSL, ARRADCOM, US Army, 1978.

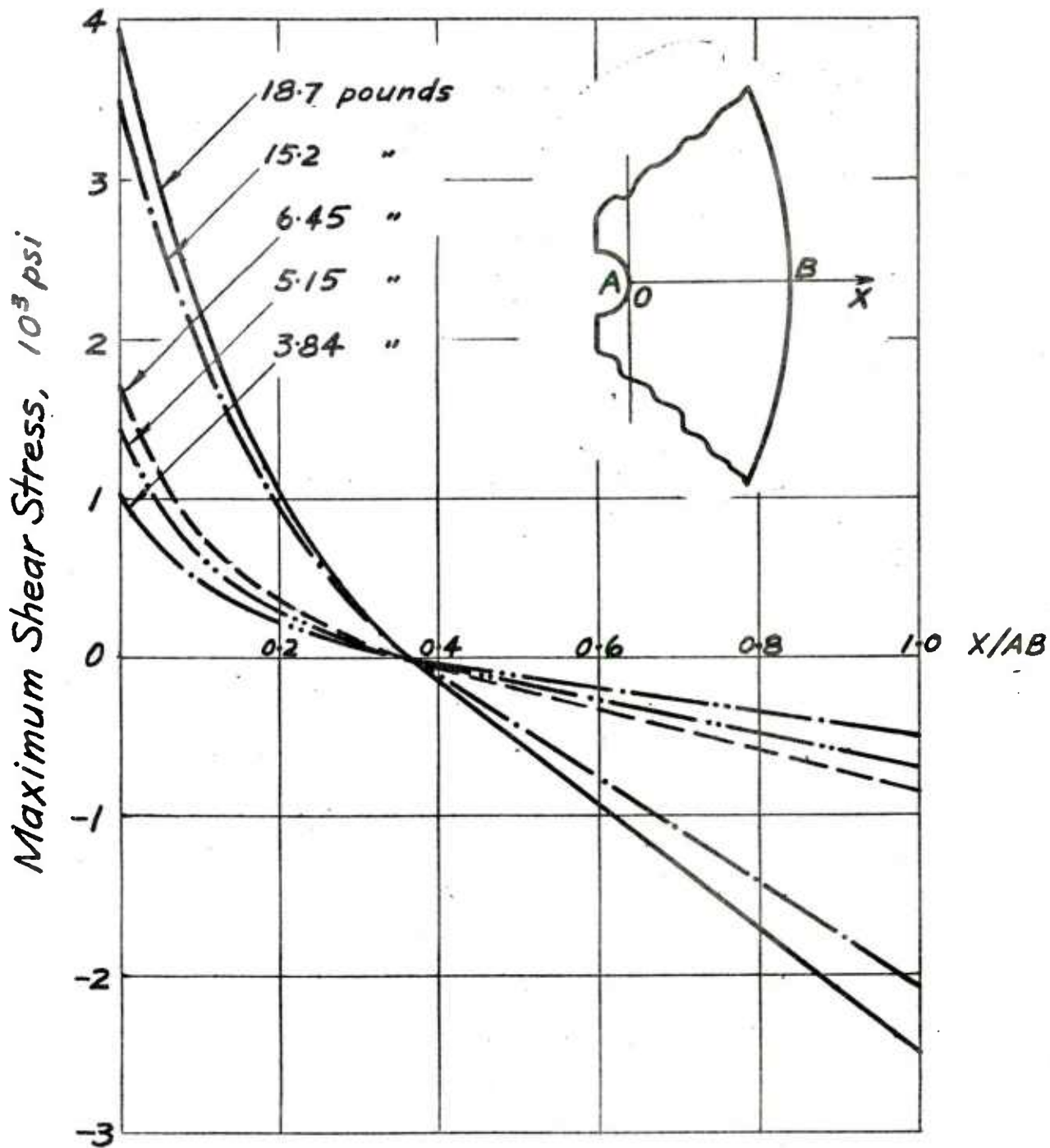


Figure 6. Maximum Shear Stress Distribution Across Section AB in C-Shaped Specimen.

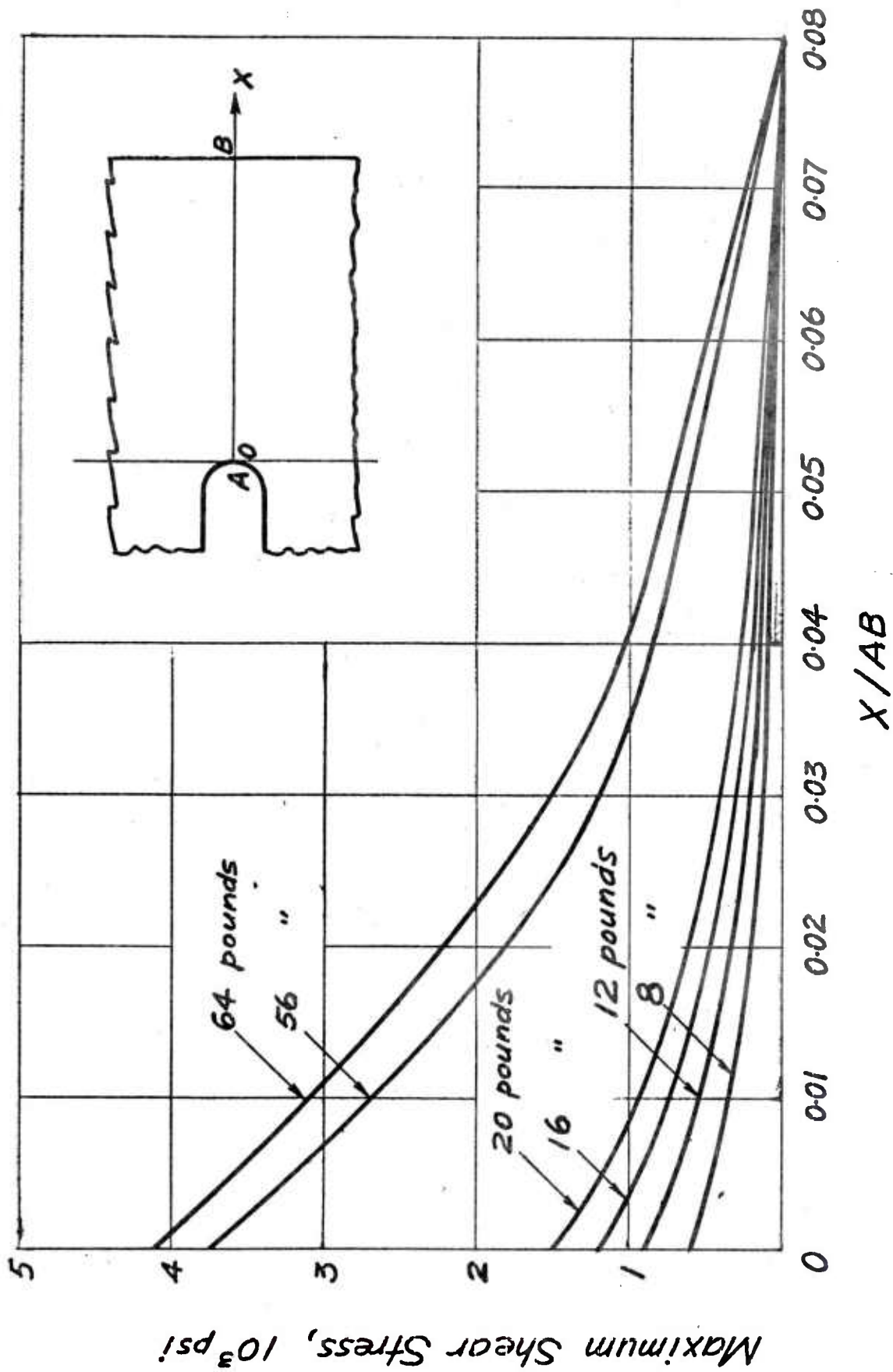


Figure 7. Maximum Shear Stress Distribution Across Part of Section AB in Compact Tensile Specimen.

Elastic Plastic Boundary

It was mentioned before that for a material obeying the yield condition of maximum shear stress, such as LEXAN, the position of elastic-plastic boundary is given by loci where the maximum shear stress reaches a value of $\sigma_y/2$.

In this investigation, we choose proportional limit stress (6.2×10^3 psi) as σ_y instead of secant yield strength (8.7×10^3 psi at $E_{\text{sec}} = 0.7E$). Hence, the elastic-plastic boundary is given by the loci where the maximum shear stress reaches 3.1×10^3 psi. For example, in the C-shaped specimen at a load of 18.7 pounds, the plastic region has penetrated from the notch root to a distance equal to 0.04 AB. Table I shows the depth of the plastic region at two levels of load for both specimens. It also shows the extended angle of plastic region along the notch boundary determined from the 7.2X fringe photographs.

Boundary Stresses and Stress Concentration Factors

On the free boundary one of the principal stresses is identically zero, and the remaining principal stress tangent to the boundary is found by converting the boundary fringe order to stress according to the stress fringe relation in Figure 4. The stress concentration factor, K , is defined as the ratio of the boundary stress to the nominal stress, equation (1). They are shown in Tables II and III.

The results show that as long as the specimen is in the elastic state, stress concentration factor K at the notch root is constant and the curve K versus σ_{nom} is straight and horizontal. However, if σ_{nom} is increased so

TABLE I. SIZE OF PLASTIC REGION

Specimen	Load (Pounds)	Plastic Region	
		Depth Along Section AB	Extended Angle Along Notch Boundary
C-shaped	15.2	.02 AB	50°
C-shaped	18.7	.04 AB	65°
Compact	56	.006 AB	70°
Compact	64	.01 AB	90°

TABLE II. STRESS CONCENTRATION FACTOR, PERCENTAGE OF OVERLOADING,
AND RESIDUAL STRESS IN C-SHAPED SPECIMEN

Load (pounds)	Nominal Stress		Boundary Stress		K_A	Stress Concentration Factor K_B	Percentage of Overloading	Residual Stress (psi)
	σ_{Ar} (psi)	σ_{Br} (psi)	σ_A (psi)	σ_B (psi)				
3.84	1350	-1250	2040	-1050	1.51	0.84		
5.15	1810	-1670	2850	-1410	1.57	0.84		
6.45	2270	-2100	3450	-1710	<u>1.52</u> Ave: 1.53	0.81		
15.2	5350	-4940	7000	-4200	1.31	0.85	32%	-1190
18.7	6580	-6080	7850	-5000	1.19	<u>0.82</u> Ave: 0.83	63%	-2220

TABLE III. STRESS CONCENTRATION FACTOR, PERCENTAGE OF OVERLOADING,
AND RESIDUAL STRESS IN THE COMPACT TENSILE SPECIMEN

Load (pound)	Nominal Stress σ_{Ap} (psi)	Boundary Stress σ_A (psi)	Stress Concentration Factor K	Percentage of Overloading	Residual Stress (psi)
8	550	1190	2.16		
12	820	1790	2.18		
16	1090	2380	2.18		
20	1370	2980	$\frac{2.18}{\text{Ave: } 2.18}$		
56	3830	7500	1.96	35	-840
64	4370	8200	1.88	54	-1330

that local yielding sets in, the stress concentration factor begins to decrease rather sharply, as shown in Figure 8.

DISCUSSIONS

Calculated Residual Stress and Percentage of Overloading

The usual assumption that unloading is inherently an elastic process is made for the purpose of calculating the residual stress after unloading. For example, in the elastic state, a load of 18.7 pounds would produce a notch root stress of $(1.53)(352)(18.7) = 10.1 \times 10^3$ psi.* Subtractive superposition of this value with 7.85×10^3 psi from elastoplastic load of 18.7 pounds gives a residual stress of 2.22×10^3 psi compression, as shown in Table II.

The proportional limit load is the load which produces a notch root stress equal to the proportional limit of the material. It is used as the basis for calculating the percentage of overloading. It can be shown that the proportional limit load for the C-shaped specimen has a value of 11.5 pounds. The percentage of overloading is $\frac{P-11.5}{11.5} \times 100\%$.

The residual stress and percentage of overloading for both specimens in the elastoplastic state were calculated and shown in Tables II and III.

*Using the real dimensions of the specimen, eq. (1) gives the nominal stress at point A a value of 352P. 1.53 is the stress concentration factor.

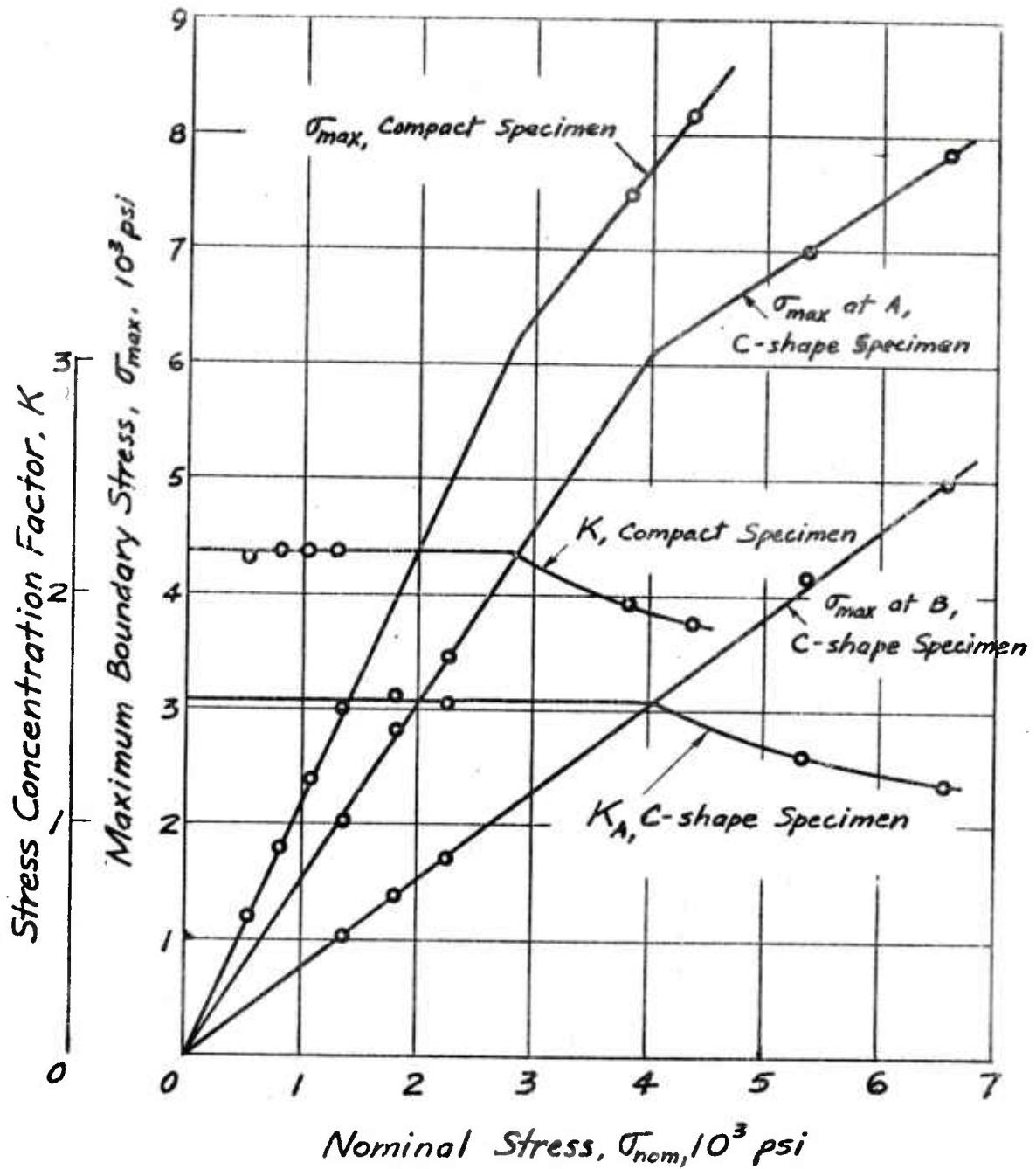


Figure 8. Curves of Stress Concentration Factor, K , and Maximum Boundary Stress, σ_{max} Versus Nominal Stress, σ_{nom} .

Stress at Point B in C-Shaped Specimens

Table II and Figure 6 show that the stress at point B in the C-shaped specimen is less than the nominal value. Hence, the stress concentration factor at B is less than one. Table II further shows that for the C-shaped specimen at 18.7 pounds of load, point B was still in the elastic state although plastic region had already penetrated from point A to a depth of 0.04 AB. Assuming that the material property in compression is the same as in tension, point B would begin to yield in compression at a load of approximately $6200/(325)(0.83) = 23$ pounds.

Transition to Prototype

In the elastic state, stress concentration factors obtained from polycarbonate model are readily applicable to specimens of other material.

In the elastoplastic state, the transition of data requires, at least, three more conditions: (a) the stress-strain curves of the materials of model and prototype must have the same shape, (b) the law of yielding must be the same for both materials, and (c) Poisson's ratio in the plastic range must be equivalent. Polycarbonate has a Poisson's ratio of 0.38 in the elastic state and 0.5 in the plastic state.⁵ It follows von Mises' yield criterion with negligible error.⁶

⁵Gurtman, G. A., Jenkins, W. C., and Tung, T. K., "Characterization of a Birefringent Material for Use in Photoelastoplasticity," Douglas Report SM-47796, Missile and Space Systems Division, Douglas Aircraft Company, February 1965.

⁶Whitfield, J. K. and Smith, C. W., "Characterization Studies of a Potential Photoelastoplastic Material," Experimental Mechanics, Vol. 12, No. 2, pp. 67-72, February 1972.

Experimental data in the elastoplastic state is transferable from polycarbonate model to any other material having the same value of Poisson's ratio and following the same law of yielding, provided the first condition is also met. The shape of stress-strain curve is represented by a parameter in the Ramberg-Osgood equation. It is possible to alter the shape of stress-strain curve of polycarbonate material by adjusting the temperature and relative humidity of the laboratory so that the curve corresponds more closely to that of a particular prototype material.

CONCLUSIONS

A photoelastoplastic investigation has been made to determine the stress concentration factors in two notched specimens of polycarbonate material. The residual stress after unloading was found by making the usual assumption that unloading is an elastic process. The results contained in this report are experimental and could be useful in verifying any analytical results.

The specimens used in another section of this laboratory were made of gun steel. Its stress-strain relation is different from that of polycarbonate material. Therefore, it is not feasible to transfer data from polycarbonate to gun steel in the elastoplastic state. It is proposed for future work to study the same problem in models made of gun steel. Birefringent coatings and reflected light polariscope can be used to determine the elastic as well as elastoplastic states of stresses on the surface of the model. The results could provide a relation between the extent of increase of fatigue life and the percentage of overloading in the gun steel model.

REFERENCES

1. Frocht, M. M., Photoelasticity, Vol. I and II, John Wiley and Sons, 1948.
2. Frocht, M. M. and Cheng, Y. F., "An Experimental Study of the Laws of Double Refraction in the Plastic State in Cellulose Nitrate - Foundations for Three Dimensional Photoelasticity," Proceedings International Symposium on Photoelasticity, pp. 195-216, 1961.
3. Ramberg, W. and Osgood, W. R., "Description of Stress Strain Curves by Three Parameters," NACA TN 902, 1943.
4. Cheng, Y. F., "A Photoelastic Study of Residual Stress in an Overloaded Breech Ring," Technical Report ARLCB-TR-78018, Benet Weapons Laboratory, LCWSL, ARRADCOM, US Army, 1978.
5. Gurtman, G. A., Jenkins, W. C., and Tung, T. K., "Characterization of a Birefringent Material for Use in Photoelastoplasticity," Douglas Report SM-47796, Missile and Space Systems Division, Douglas Aircraft Company, February 1965.
6. Whitfield, J. K. and Smith, C. W., "Characterization Studies of a Potential Photoelastoplastic Material," Experimental Mechanics, Vol. 12, No. 2, pp. 67-72, February 1972.

TECHNICAL REPORT INTERNAL DISTRIBUTION LIST

	<u>NO. OF COPIES</u>
COMMANDER	1
CHIEF, DEVELOPMENT ENGINEERING BRANCH	1
ATTN: DRDAR-LCB-DA	1
-DM	1
-DP	1
-DR	1
-DS	1
-DC	1
CHIEF, ENGINEERING SUPPORT BRANCH	1
ATTN: DRDAR-LCB-SE	1
-SA	1
CHIEF, RESEARCH BRANCH	2
ATTN: DRDAR-LCB-RA	1
-RC	1
-RM	1
-RP	1
CHIEF, LWC MORTAR SYS. OFC.	1
ATTN: DRDAR- LCB-M	1
CHIEF, IMP. 81MM MORTAR OFC.	1
ATTN: DRDAR- LCB-I	1
TECHNICAL LIBRARY	5
ATTN: DRDAR- LCB-TL	
TECHNICAL PUBLICATIONS & EDITING UNIT	2
ATTN: DRDAR- LCB-TL	
DIRECTOR, OPERATIONS DIRECTORATE	1
DIRECTOR, PROCUREMENT DIRECTORATE	1
DIRECTOR, PRODUCE ASSURANCE DIRECTORATE	1

NOTE: PLEASE NOTIFY ASSOC. DIRECTOR, BENET WEAPONS LABORATORY, ATTN:
DRDAR- LCB-TL, OF ANY REQUIRED CHANGES.

TECHNICAL REPORT EXTERNAL DISTRIBUTION LIST

	<u>NO. OF COPIES</u>		<u>NO. OF COPIES</u>
ASST SEC OF THE ARMY RESEARCH & DEVELOPMENT ATTN: DEP FOR SCI & TECH THE PENTAGON WASHINGTON, D.C. 20315	1	COMMANDER US ARMY TANK-AUTMV R&D COMD ATTN: TECH LIB - DRDTA-UL MAT LAB - DRDTA-RK WARREN MICHIGAN 48090	1 1
COMMANDER US ARMY MAT DEV & READ. COMD ATTN: DRCDL 5001 EISENHOWER AVE ALEXANDRIA, VA 22333	1	COMMANDER US MILITARY ACADEMY ATTN: CHMN, MECH ENGR DEPT WEST POINT, NY 10996	1
COMMANDER US ARMY ARRADCOM ATTN: DRDAR-IC	1	COMMANDER REDSTONE ARSENAL ATTN: DRSMI-RB	2
-ICA (PLASTICS TECH EVAL CEN)	1	-RRS	1
-LCE	1	-RSM	1
-LCM	1	ALABAMA 35809	
-LCS	1	COMMANDER ROCK ISLAND ARSENAL	
-LCW	1	ATTN: SARRI-ENM (MAT SCI DIV)	1
-TSS(STINFO)	2	ROCK ISLAND, IL 61202	
DOVER, NJ 07801		COMMANDER HQ, US ARMY AVN SCH ATTN: OFC OF THE LIBRARIAN	1
COMMANDER US ARMY ARRCOM ATTN: DRDAR-LEP-L	1	FT RUCKER, ALABAMA 36362	
ROCK ISLAND ARSENAL ROCK ISLAND, IL 61299		COMMANDER US ARMY FGN SCIENCE & TECH CEN ATTN: DRXST-SD	1
DIRECTOR US Army Ballistic Research Laboratory ATTN: DRDAR-TSB-S (STINFO)	1	220 7TH STREET, N.E. CHARLOTTESVILLE, VA 22901	
ABERDEEN PROVING GROUND, MD 21005		COMMANDER US ARMY MATERIALS & MECHANICS RESEARCH CENTER	
COMMANDER US ARMY ELECTRONICS COMD ATTN: TECH LIB	1	ATTN: TECH LIB - DRXMR-PL	2
FT MONMOUTH, NJ 07703		WATERTOWN, MASS 02172	
COMMANDER US ARMY MOBILITY EQUIP R&D COMD ATTN: TECH LIB	1		
FT BELVOIR, VA 22060			

NOTE: PLEASE NOTIFY COMMANDER, ARRADCOM, ATTN: BENET WEAPONS LABORATORY, DRDAR-LCB-TL, WATERVLIET ARSENAL, WATERVLIET, N.Y. 12189, OF ANY REQUIRED CHANGES.

TECHNICAL REPORT EXTERNAL DISTRIBUTION LIST (CONT)

	<u>NO. OF COPIES</u>		<u>NO. OF COPIES</u>
COMMANDER US ARMY RESEARCH OFFICE P.O. BOX 12211 RESEARCH TRIANGLE PARK, NC 27709	1	COMMANDER DEFENSE TECHNICAL INFO CENTER ATTN: DTIA-TCA CAMERON STATION ALEXANDRIA, VA 22314	12
COMMANDER US ARMY HARRY DIAMOND LAB ATTN: TECH LIB 2800 POWDER MILL ROAD ADELPHIA, MD 20783	1	METALS & CERAMICS INFO CEN BATTELLE COLUMBUS LAB 505 KING AVE COLUMBUS, OHIO 43201	1
DIRECTOR US ARMY INDUSTRIAL BASE ENG ACT ATTN: DRXPE-MT ROCK ISLAND, IL 61201	1	MECHANICAL PROPERTIES DATA CTR BATTELLE COLUMBUS LAB 505 KING AVE COLUMBUS, OHIO 43201	1
CHIEF, MATERIALS BRANCH US ARMY R&S GROUP, EUR BOX 65, FPO N.Y. 09510	1	MATERIEL SYSTEMS ANALYSIS ACTV ATTN: DRXSY-MP ABERDEEN PROVING GROUND MARYLAND 21005	1
COMMANDER NAVAL SURFACE WEAPONS CEN ATTN: CHIEF, MAT SCIENCE DIV DAHLGREN, VA 22448	1		
DIRECTOR US NAVAL RESEARCH LAB ATTN: DIR, MECH DIV CODE 26-27 (DOC LIB) WASHINGTON, D. C. 20375	1 1		
NASA SCIENTIFIC & TECH INFO FAC P. O. BOX 8757, ATTN: ACQ BR BALTIMORE/WASHINGTON INTL AIRPORT MARYLAND 21240	1		

NOTE: PLEASE NOTIFY COMMANDER, ARRADCOM, ATTN: BENET WEAPONS LABORATORY, DRDAR-ICB-TL, WATERVLIET ARSENAL, WATERVLIET, N.Y. 12189, OF ANY REQUIRED CHANGES.